arXiv:1510.08299v1 [physics.bio-ph] 28 Oct 2015

Active mechanics reveal molecular-scale force kinetics in living oocytes

Wylie W. Ahmed[1,*], Etienne Fodor[2,*], Maria Almonacid[3,*], Matthias Bussonnier[1], Marie-Helene Verlhac[3], Nir S. Gov[4], Paolo Visco[2], Frederic van Wijland[2], and Timo Betz[1]

[1]*Institut Curie, Centre de recherche, 11, rue Pierre et Marie Curie, 75005 Paris, France; Sorbonne Universites, Universite Pierre et Marie Curie, Paris, France; Centre National de la Recherche Scientifique, UMR168, Paris, France.*

[2]*Laboratoire Matiere et Systemes Complexes, UMR 7057, Universite Paris Diderot, 75013 Paris, France*

[3]*CIRB, College de France, and CNRS-UMR7241 and INSERM-U1050, Equipe Labellisee Ligue Contre le Cancer, Paris F-75005, France.*

[4]*Department of Chemical Physics, Weizmann Institute of Science, 76100 Rehovot, Israel*

[*]*equally contributing authors*

October 29, 2015

Abstract

Unlike traditional materials, living cells actively generate forces at the molecular scale that change their structure and mechanical properties. This nonequilibrium activity is essential for cellular function, and drives processes such as cell division. Single molecule studies have uncovered the detailed force kinetics of isolated motor proteins in-vitro, however their behavior in-vivo has been elusive due to the complex environment inside the cell. Here, we quantify active force generation in living oocytes using in-vivo optical trapping and laser interferometry of endogenous vesicles. We integrate an experimental and theoretical framework to connect mesoscopic measurements of nonequilibrium properties to the underlying molecular-scale force kinetics. Our results show that force generation by myosin-V drives the cytoplasmic-skeleton out-of-equilibrium (at frequencies below 300 Hz) and actively softens the environment. In vivo myosin-V activity generates a force of $F \sim 0.4$ pN, with a power-stroke of length $\Delta x \sim 20$ nm and duration $\tau \sim 300$ μs, that drives vesicle motion at $v_{\mathrm{v}} \sim 320$ nm/s. This framework is widely applicable to quantify nonequilibrium properties of living cells and other soft active materials.

1 Introduction

Living cells utilize motor proteins to actively generate force at the molecular scale to drive motion and organization in the crowded intracellular environment [1, 2, 3, 4]. For example, force generation is critical to facilitate the basic tasks of living cells such as spatial organization, motility, division, and vesicle transport. Non-living systems in thermal equilibrium also self-organize, which can often be explained by minimization of energy [5]. However, self-organization is also observed in far-from-equilibrium systems such as driven colloids [6], molecular motors [7], and living cells [8], but the underlying physics is not well understood. Biology is full of many striking examples of far-from-equilibrium self-organization [9, 10].

An interesting example occurs during early vertebrate development, namely oocyte meiosis. Oocytes are immature female gametes that are destined to be fertilized and grow into a fully functioning organism. They are very large cells (80 μm in diameter) of spherical geometry with a thick cortex and a well separated cytoplasmic-skeleton (Fig. 1A). The cytoplasmic-skeleton of a mouse oocyte is a composite material that includes actin filaments, microtubules, and intermediate filaments. The actin network is composed of long unbranched filaments polymerized from the surface of vesicles that harbor actin nucleating factors [11]. These vesicles act as nodes to create an inter-connected actin network that is uniform in density throughout the cytoplasm and not polarized [12]; Microtubules are organized in small seeds and do not form long filaments during prophase I [13]; And while it is probable that intermediate filaments are present [14], little is known about their structure or function in mouse oocytes.

The interior of the oocyte is highly dynamic due mainly to an active F-actin network, nucleated by Formin-2 [15, 12]. During their development, oocytes must move large intracellular structures such as the meiotic spindle in preparation for fertilization [16, 17]. When oocytes undergo asymmetric division they actively transport their meiotic spindle to one side of the cell to facilitate splitting of chromosomes while retaining sufficient storage material for development [18]. This requires precise spatial and temporal coordination of the cytoskeleton and molecular motors [19, 12]. Recent work has shown the importance of mechanical processes in oocyte development [19, 12, 20]. Proper spindle positioning requires the oocyte cortex to soften and exhibit plastic deformation [19], and motion of the cytoplasmic actin network is closely regulated by myosin-V motors [12]. Motion of large objects, such as positioning of the spindle[19] or nucleus [20], must be driven by a physical force. In this study, we directly quantify the nonequilibrium activity and extract the molecular-scale forces generated by the actin-myosin-V network that drive cytoplasmic vesicle motion.

From the material science point-of-view, oocytes are an encapsulated polymer droplet filled with colloidal particles actively driven by their surrounding medium. This forms an active soft material that is maintained in a far-from-equilibrium state, providing a well-suited system to study nonequilibrium physics. From the biological point-of-view, oocytes are the precursor for development of all complex organisms, but much of their inner-workings remain a mystery due to lack of quantitative measurements of activity and behavior.

To investigate the nonequilibrium mechanical activity in living cells, it is necessary to independently measure the active molecular force generation and the mechanical properties of the local area to understand how objects navigate the complex intracellular environment. This methodology was introduced to study active processes in hair bundles [21] and stress fluctuations in cells [22]. Subsequent studies utilized this concept to

investigate cross-linked actin-myosin-II networks in reconstituted systems [23] and beads embedded in living cells [24, 25, 26, 27].

We measure the out-of-equilibrium motion (activity) of endogenous vesicles in the largely unexplored cytoplasmic-skeleton of in-vivo mouse oocytes and develop a theoretical model to account for strong viscoelastic effects that quantifies the driving forces. We combine optical tweezer based active microrheology (AMR) and laser-tracking interferometry with our theoretical framework to quantify the in-vivo active mechanics and relate them to the underlying force kinetics. To study the activity of the actin-myosin-V network, we examine the cytoplasmic-skeleton of mouse oocytes in prophase-I. While this network is the key element in nuclear positioning [20], the underlying physical processes are not well understood. By using statistical mesoscopic measurements on in-situ vesicles, and theoretical modeling, we are able to extract the molecular-scale force kinetics (power-stroke duration and length, force, and velocity) of myosin-V. Our results demonstrate that nonequilibrium activity of the actin-myosin-V network is the dominant mechanism that drives active motion and determines the mechanical properties in the oocyte.

2 Results

2.1 Intracellular mechanics of the cytoplasmic-skeleton

To measure the local mechanical properties, we optically trap an endogenous vesicle embedded in the cytoplasmic-skeleton, apply an oscillatory force while measuring its displacement (Fig 1B), and calculate the shear modulus via the Generalized Stokes-Einstein relation [28]. Since vesicles serve as integrated nodes in the cytoplasmic-skeleton, they accurately reflect the mechanics and fluctuations of the network [29]. To calibrate the force on the vesicles we exploit the established observation that high-frequency fluctuations are thermal in origin [30, 24, 31]. AMR directly measures the complex modulus (G^*) characterizing the viscous and elastic resistance of the composite cytoplasmic-skeleton including any contribution from actin, intermediate filaments, microtubules, and other structures present. We find that the cytoplasmic-skeleton of oocytes has strongly viscoelastic properties similar to semiflexible biopolymer networks [32, 33], exhibiting the high-frequency power-law behavior ($G^* \propto f^\alpha$, where $\alpha \sim 0.75$). This mechanical behavior is similar to that of reconstituted networks of entangled actin filaments, but significantly stiffer (Fig 1C). Thus, the cytoplasmic-skeleton in oocytes is strongly frequency dependent, which must be accounted for when modeling its mechanical behavior.

To dissect the mechanical contributions of cytoskeletal filaments in oocytes we first perform AMR on oocytes that lack cytoplasmic actin filaments nucleated by formin-2 (Fmn -/-). We find that the mechanical properties do not change compared to WT, indicating that the actin network does not provide significant mechanical resistance in the oocyte (Fig 2A, B). This behavior is presumably because the actin network in WT oocytes is sparse (Fig 1A, right and Fig. S3) with a mesh size of $5.7 \pm 1.9\mu$m [17]. To check this, we examine in-vitro reconstituted actin networks with a mesh size of ~ 200 nm [34], which were found to be an order of magnitude softer than the oocyte (Fig 1C), thus supporting the result that WT oocyte mechanics is not dominated by the actin cytoskeleton. Depolymerizing the microtubules by nocodazole treatment (1 μM) does not significantly affect the mechanical properties (Fig. 2A, B). Indicating that microtubules also do not provide significant mechanical resistance in the cytoplasmic-skeleton. This result is expected since prophase I microtubules form small seeds instead of long force-bearing tubule structures [13]. These combined results suggest that there are other force-bearing structures in the cytoplasm of mouse oocytes.

While our results show that actin does not contribute significantly to the mechanical resistance, it is known that the actin-myosin-V meshwork activity plays a critical role for self-organization such as positioning of the meiotic spindle [16, 17] and nucleus centering in mouse oocytes [20]. To independently probe the activity of this network we impaired the myosin-V motor force generation by de-activating it via microinjection of a dominant negative construct (MyoV(-))[11, 20] (see Materials and Methods). The MyoV(-) construct targets the dimerization domain of endogenous myosin-Vb, which is still able to bind vesicles and actin, but no longer allows dimerization and active force generation. When myosin-V activity is absent, the mechanical properties of the cytoplasmic-skeleton stiffens significantly as evidenced by the shift upwards in the elastic and viscous moduli (Fig 2A, B). This increased mechanical stiffness correlates with a higher density actin meshwork that is observed in the absence of myosin-V activity (Fig. S3 in SI) and could be related to increased cross-linking [12]. This result highlights how cellular activity can be used to tune mechanical properties.

The overall behavior of the cytosplasmic-skeleton in oocytes is strongly viscoelastic where neither the elastic or viscous components dominate by a large margin. At lower frequencies the behavior is slightly more elastic with a crossover ($\sim 10 - 20$ Hz) to more viscous at higher frequencies. However both components of the shear moduli are always within a factor of two at the observed frequencies (Fig. 2C).

2.2 Quantifying nonequilibrium mechanical activity

To quantify nonequilibrium activity we use laser-tracking to precisely measure the spontaneous motion of vesicles in the cytoplasmic-skeleton with high spatio-temporal resolution [35, 36, 37] (see Materials and Methods). Both the spontaneous motion and the local mechanics are measured for each individual vesicle. This allows direct comparison between the local environment experienced by the vesicle and the motor activity that is driving its motion. This is critical in order to extract information about the molecular-scale processes. In the absence of biochemical activity the motion of the vesicles would be due to purely thermal agitation, which is fully determined by the mechanical properties of the system. This basic relation is given by a fundamental theorem of statistical mechanics known as the fluctuation-dissipation theorem (FDT) [38]. The FDT relates the small fluctuating motion of the vesicles to the mechanical properties of the surrounding environment by, $\tilde{\chi}'' = \pi f \tilde{C}/k_B T$, where $\tilde{\chi}''$ is the dissipative part of the mechanical response, $\tilde{C}$ is the power spectral density of vesicle motion, f is frequency, and $k_B T$ is thermal energy. However, in living cells the presence of biochemical activity gives rise to active forces (e.g. a nonequilibrium process) driven by energy consuming processes [21, 22, 39]. In other words, the force driving the motion of particles in a living cell (e.g. the oocyte) has two contributions: (1) a passive (purely thermal) contribution described by classical equilibrium physics; (2) an active contribution that is biochemically regulated and cannot be understood via equilibrium physics.

We quantify and explain both the passive and active contributions driving intracellular fluctuations, by independently measuring each side of the FDT. We use AMR to measure $\tilde{\chi}$ and laser-tracking to measure $\tilde{C}$, and use this information to check for violation of FDT [23, 21, 40], which indicates active force generation. In oocytes, at high-frequencies the mechanical response ($\tilde{\chi}''$) and the spontaneous vesicle motion ($\pi f \tilde{C}/k_B T$) are equal as expected for thermal fluctuations [30, 24] (Fig. 3A). At frequencies below ~ 300 Hz, the observed motion of vesicles is dominated by an active energy consuming process (highlighted by the pink shaded region between the two curves in Fig 3A).

To quantify the nonequilibrium activity in an active soft material it is instructive to consider the effective energy [21, 41, 42, 43], $E_{\text{eff}} = \pi f \tilde{C}/\tilde{\chi}''$, which is a measure of how far the system is from thermal equilibrium. WT oocytes exhibit the strongest departure from equilibrium due to the actin-myosin-V network activity. Accordingly, the deviation is reduced when either actin is absent (Fmn -/-) or myosin-V is inactivated (MyoV (-)) (Fig 3B). This is quantitative confirmation that the dynamic actin-myosin-V meshwork drives vesicle dynamics out-of-equilibrium in the cytoplasmic-skeleton of mouse oocytes [12, 20]. Additionally, this demonstrates that other sources of activity remain in the living oocyte since non-thermal activity is still evident.

To develop a more intuitive picture of the activity we quantify the forces generated in the cell by calculating the cell force spectrum (S_{cell}) [22, 24, 25, 40]. S_{cell} directly represents the total forces on vesicles from all stochastic sources (active and thermal) inside the cell. In analogy to the force on a simple spring, where the force is the stiffness $\times$ displacement ($F = \kappa \Delta x$, where κ is stiffness and Δx is displacement), we calculate $S_{\text{cell}} \propto |G^*|^2 \tilde{C}$ where $|G^*|^2$ is the stiffness of the cytoplasmic-skeleton and $\tilde{C}$ is the spontaneous displacement of the vesicle [24, 25, 44]. In our framework we separate the total force spectrum in the cell to be the sum of thermal forces and active forces ($S_{\text{cell}} = S_{\text{therm}} + S_{\text{active}}$) [45, 40]. As an illustration of this separation of thermal and active forces we show a representative trajectory of a vesicle (Fig. 3E, black). Based on our measured violation of FDT (Fig. 3A), we isolate the low-frequency vesicle motion which is due to active processes and the high-frequency motion that is dominated by thermal motion (Fig. 3E green, F respectively). The resulting force spectrum is shown in Fig 3C where at high frequencies the cell force spectrum (S_{cell}) is dominated by thermal forces (where $S_{\text{active}} \ll S_{\text{thermal}}$) as expected, but at lower frequencies ($f < 300$ Hz) active forces exist ($S_{\text{active}} \gg S_{\text{thermal}}$) which result in higher total force experienced by vesicles in the cytoplasm over thermal equilibrium (lines represent theoretical model). The cell force spectrum, S_{cell} quantifies the average stochastic force experienced by a vesicle in the cytoplasmic-skeleton.

2.3 Modeling active force fluctuations

Myosin-V is typically considered a cargo transport motor. However, in prophase-I mouse oocytes, myosin-V drives vesicle motion in a non-directed fashion as evidenced by its sub-linear scaling of the mean-squared-displacement (Fig. 3D, blue). Previous work has also showed that myosin-V drives random motion of vesicles (active diffusion) on longer timecales of minutes [20]. To further illustrate this point, Fig. 4A(left) shows vesicles and actin filaments embedded in the oocyte interior. The complex mechanical environment is represented by a generic continuum (gray background). When myosin-V is attached to a vesicle and applies force on an actin filament, this force is transduced through the actin filament to a neighboring vesicle where it is bound by formin-2 (e.g. black arrows in Fig. 4A, right). This process occurs frequently throughout the oocyte interior resulting in randomly distributed force-dipoles (similar to myosin-II in some systems [30, 23]). Thus, each vesicle experiences forces in random directions due to the action of myosin-V throughout the network. This is represented by many actin filaments under force as shown in magenta in Fig. 4A(right). Therefore, due to the unique network connectivity in the cytoplasmic-skeleton, myosin-V motors drive active random motion in prophase-I mouse oocytes reminiscent of cytoplasmic stirring observed previously that was driven by myosin-II [30].

To gain access to the molecular-scale kinetics of the active processes driving the polymeric interior of oocytes we developed a quantitative model describing vesicles embedded in a viscoelastic environment that are subjected to thermal and active forces. Here, the nonequilibrium processes, such as molecular motor activity, provide the active forces that reorganize the polymer cytoskeleton and drive motion of the vesicles. Our theoretical framework extends previous approaches for near-elastic networks [46, 44, 40] to include the complex mechanical properties measured experimentally (Fig 2). The model describes a vesicle that is freely fluctuating in the viscoelastic continuum due to thermal forces, experiencing a local confinement illustrated by the harmonic potential, with stiffness κ, in Fig. 4B(left) and governed by the dynamics described in equation 1. The molecular motor activity injects random forces into the network, which results in an active force f_A on the vesicle that drives it to a new equilibrium position x_0 as in Fig. 4B(right) described by equation 2. These coupled equations of motion written in the Generalized Langevin approach describe vesicle motion in the active viscoelastic environment of the cytoplasmic-skeleton,

$$\int^t \mathrm{d}t' \gamma(t-t') \frac{\mathrm{d}x}{\mathrm{d}t} = -\kappa(x - x_0) + \xi \tag{1}$$

$$\int^t \mathrm{d}t' \gamma(t-t') \frac{\mathrm{d}x_0}{\mathrm{d}t} = \kappa \zeta_\alpha v_\mathrm{A} \tag{2}$$

where ξ is Gaussian colored noise representing thermal forces, κ is the local confinement, γ is the memory kernel, ζ_α is the microscopic timescale describing the mechanical properties of the cytoplasmic-skeleton, v_A is the velocity of the stochastic active force, and x is the vesicle position. To account for the mechanical behavior of the cytoplasmic-skeleton that was measured by AMR, a power-law form of the memory kernel is utilized to describe the viscoelastic properties (details in SI). This model can directly separate the passive forces that originate from the thermal fluctuations of the medium and the active forces that depend on the the energy consuming processes in the active material. Note that if the active force ($f_A = \kappa\zeta_\alpha v_\mathrm{A}$) is zero, then equation 2 is zero, and the equation of motion simplifies to the usual viscoelastic Brownian motion (equation 1). If the active force is not zero, then it originates from molecular motor activity that has step-like velocity kinetics (Fig 4B, right inset). Endogenous vesicles experience an effective force kick of average duration τ followed by a quiescent period of average duration τ_0 [44, 40]. These force kicks drive the nonequilibrium fluctuations in our model.

2.4 Extracting molecular-scale force kinetics

By combining our model and experimental measurements, we can extract the force kinetics driving nonequilibrium mechanical processes in the oocyte. The active force spectrum represents the average force experi-

enced by the vesicles due only to active processes, and can be expressed as

$$S_{\text{active}} = \underbrace{\frac{1}{(2\pi f\zeta_\alpha)^{2\alpha}}}_{\text{mechanics}} \underbrace{\frac{1}{1+(2\pi f\tau)^2} \frac{2(F\zeta_\alpha)^2}{3(\tau+\tau_0)}}_{\text{motor activity}} \tag{3}$$

where ζ_α and α reflect the viscoelastic material properties of timescale and frequency dependence, F is the apparent active force amplitude, τ is the average time of force application, and τ_0 is the average time between force kicks (Fig. 4B, right inset). The first term in equation 3 depends on the mechanical properties of the cytoplasmic-skeleton and the second term is related to the kinetic properties of the active processes. This illustrates that the active force spectrum is dependent on the force generation by molecular motors as well as the mechanics of the environment that they must push against. The power-law scaling of the active force spectrum contains information about the underlying physics. At lower frequencies the active force spectrum scales as $f^{-2\alpha}$ reflecting the active forces pushing against the viscoelastic environment. At higher frequencies the active force spectrum provides information on the molecular kinetics of the active force generation process which scales as $f^{-(2\alpha+2)}$. Our predicted active force spectrum exhibits power-law scaling that is dependent on the mechanical properties of the system (α), in contrast to previous studies [46, 22, 47]. Previous theoretical developments predict an active force spectrum with slope of -2 that is independent of the mechanical properties [22] and a plateau (slope of 0) below a critical frequency (equation 2 in [30] and equation S1 in [24]). It is worth noting that in the near-elastic case ($\alpha \sim 0$), our model recovers the behavior observed in previous work [24, 30]. The divergence of the active force spectrum at low frequencies is consistent with our experimental measurements, and others, where a low-frequency plateau is not observed [27, 25, 48, 24, 49].

The experimental measurements for the active force spectrum ($S_{\text{active}} = S_{\text{cell}} - S_{\text{therm}}$) and theoretical model are compared in Fig 4C. The low frequency power-law behavior is clearly seen, while at higher frequencies the active forces drop off rapidly which reflects the molecular motor statistics [50]. This drop-off of the active force spectrum allows extraction of τ, the timescale of active force application. Without additional assumptions, all subsequent molecular-scale force kinetics are now constrained by our model and can be calculated, such as the apparent active force amplitude,

$$F = [3\kappa k_B T_A(\tau+\tau_0)/\zeta_\alpha]^{1/2} \tag{4}$$

where $k_B T_A$ defines the active energy scale (see SI for details). The apparent force amplitude, F, is the average active force that the endogenous vesicle feels that drives its motion. Once this force is known it is straight-forward to calculate the expected average vesicle velocity,

$$v_{\text{v}} = \frac{F}{\kappa\zeta_\alpha} \tag{5}$$

which is a ratio of the driving force, F, and the resistance provided by the surrounding environment, $\kappa\zeta_\alpha$. Following this argument an approximate step-size of the force kick can be computed by $\Delta x = F/\kappa$. Thus, once the timescale of the force kick (τ) is extracted from equation 3, the apparent force felt by the vesicle (F), the expected vesicle velocity (v_{v}), and the step-size Δx can be deduced directly.

A main result of our combined experimental and theoretical framework is access to the molecular-scale kinetics via mesoscopic measurements of the active force spectrum. In living oocytes we find that endogenous vesicles experience a force of $F \sim 0.4$ pN during a power-stroke of $\tau \sim 300$ μs duration, with a step-size of $\Delta x \sim 20$ nm, which is strikingly similar to single molecule myosin-V kinetics measured in-vitro [51, 52, 50, 53, 54, 55, 56]. In addition, we find that the predicted average vesicle velocity due to molecular motors is $v_{\text{v}} \sim 320$ nm/s which is in agreement with myosin-V velocity in vitro [51, 53, 54], as well as the velocity of myosin-V driven vesicles measured in in-vivo oocytes [20, 11]. Together, our results reveal that force kinetics of myosin-V motors are remarkably similar in in-vitro single-molecule studies and in in-vivo oocytes where they drive the composite cytoplasmic-skeleton out-of-equilibrium.

The agreement between our experiments and analytic theory indicate that the model is able to capture the nonequilibrium force fluctuations of endogenous vesicles in the cytoplasmic-skeleton of living oocytes. However, this does not guarantee that it adequately describes the overall motion of the vesicles (including higher-order statistics). To further compare our experiments and theory we use the measured parameters

(mechanics, kinetics, etc.) extracted from the force spectrum to simulate vesicle dynamics via a stochastic equation of motion (see SI). These simulations of vesicle motion use exclusively values measured from experiment, without any free parameters. We find that the statistics of the simulated vesicle motion is in excellent agreement with the measured spontaneous motion of vesicles in living oocytes as is shown by their displacement correlations (Fig 4D). Measured and simulated motion of vesicles is nearly identical including the central Gaussian region and the non-Gaussian tails (shaded red in Fig 4D) at short timescales which are indicative of molecular motor activity [57]. While our analytic model describes the mean values of the experimental measurements, these simulations exploit the full range of data by capturing the entire distribution of displacement correlations. Hence, the agreement found between simulations and experiment is non-trivial and can be considered a predictive test of the model. These results show that our model of step-like active forces is able to capture the overall motion of vesicles (including higher-order statistics) embedded in the cytoplasmic-skeleton of living oocytes.

3 Discussion

3.1 The cytoplasmic-skeleton is softened by nonequilibrium fluctuations

Our mechanical measurements (AMR) indicate that myosin-V driven nonequilibrium fluctuations maintain a softer cytoplasmic-skeleton in oocytes. The mechanism of how this occurs is not yet clear but is likely related to the structural connectivity of the actin-myosin-V network. The sparsely connected network of long unbranched actin filaments connected by myosin-V positive vesicles in oocytes exhibits a unique architecture. This active actin-myosin-V network drives random nonequilibrium fluctuations of the entire composite cytoskeleton. Repeated deformation of the composite cytoskeleton may lead to breakages resulting in softening of the overall mechanical properties. In polymer physics this behavior is known as the classical Mullins effect [58], where small amplitude cyclic strain application leads to softening. This effect has been observed in actin networks with low cross-linking density [59] and motor-mediated breakage of actin filaments has been observed in-vitro [60]. Thus, it is possible that repeated deformation due to myosin-V force generation causes the observed difference in actin density between WT and MyoV(-) (Figure S3 in SI) due to rupture or breakage of filaments/cross-links [60, 61, 62]. The motor-mediated softening reported here has also been observed due to myosin-II in suspended cells in-vitro [63], which is in constrast to the stiffening reported in adherent cells [24, 64]. The origin of softening/stiffening behavior in cells is not yet understood, but may be related to adhesion with the surrounding environment.

3.2 Nonequilibrium activity dominates below 300 Hz

In mouse oocytes, nonequilibrium activity emerges at higher frequencies ($f < 300$ Hz) than observed previously in other active systems ($f < 10$ Hz)[23, 24, 30]. This observation is not surprising since the timescale of FDT violation depends on both the mechanical properties and the typical timescale of the nonequilibrium activity of the system. The cytoplasmic-skeleton in oocytes is softer than previous systems [23, 65], and thus it is expected for the crossover to thermal motion to occur at higher frequencies (Fig S2 in SI). Additionally, myosin-V kinetics are known to be faster than myosin-II [66], which was the driving force in previous experiments [23, 24, 30].

3.3 Active force spectrum reveals molecular-scale kinetics

A significant advance represented by this work is the connection between mesoscopic measurement of nonequilibrium vesicle motion and the underlying molecular-scale driving forces in a strongly viscoelastic in-vivo system. A global fit of our theoretical model to the ensemble averaged active force spectrum reveals molecular-scale kinetics in agreement for myosin-V measured in single molecule in-vitro experiments [50, 51, 52, 53, 55, 56, 54]. It is striking that our in-vivo measurements are in such close agreement with single-molecule studies given that the crowded in-vivo environment is far more complex. To capture this behavior it was necessary to extend our theoretical framework to account for strong viscoelastic memory effects. This is most clearly seen in the low-frequency power-law scaling of the active force spectrum. Previous models predict that the active force spectrum is proportional to f^{-2} [22, 46, 40] which is able to

predict measurements made in nearly elastic systems [24, 30]. However, this behavior is not consistent with our measurements in oocytes where we observe a scaling of $f^{-4/3}$ (Fig. 4B). Our model, predicts a low-frequency behavior of $S_{\text{active}} \propto f^{-2\alpha}$ which agrees with our experimental measurement $\alpha \sim 2/3$. This shows that including the strong viscoelastic memory effects of the mechanical properties is necessary to capture the nonequilibrium properties of the cytoplasmic-skeleton in mouse oocytes. This is likely the case for any cells that cannot be considered near-elastic.

Our model allows extracts the molecular-scale force kinetics directly from fitting the active force spectrum. As a result, we are able to capture the short timescale power-stroke of the active process, which is not be possible from fitting the long timescale plateau of the MSD as done previously [24, 30]. Furthermore, we predict the force, step-size, and velocity without any further model assumptions. All resulting kinetics extracted from in-vivo oocytes are in striking agreement with single-molecule kinetics measured in-vitro as summarized in Table 1. Our approach is a versatile method to access the molecular-scale force dynamics in living cells and other soft active materials.

[Table 1 about here.]

4 Conclusion

We have demonstrated the quantification of nonequilibrium properties and molecular-scale kinetics inside the cytoplasmic-skeleton of in-vivo mouse oocytes via experiments, theory, and simulation. We find that active forces can tune the mechanical properties and the nonequilibrium fluctuations of the active polymeric interior of oocytes. Through our theoretical model we access the molecular-scale force kinetics that are driving activity in the cytoplasmic-skeleton. From the material science perspective, this is a striking example of how active materials fundamentally differ from passive materials, since their microscopic dynamics are actively tuned. From a biological perspective, nonequilibrium fluctuations are important to maintain cell functionality and mesoscopic measurements provide access to molecular-scale kinetics. Our results combine concepts from equilibrium and nonequilibrium physics to reveal that myosin-V activity is remarkably similar in-vivo as in-vitro, and that their kinetics can be extracted via measurements of cytoplasmic fluctuations.

5 Materials and Methods

5.1 Oocyte Preparation

Oocytes were collected from 11 week old mice OF1, 13 week old C57BL6 (WT) or 15 week old Fmn2 -/- female mice as previously described [67] and maintained in Prophase I arrest in M2+BSA medium supplemented with 1 μM Milrinone [68]. Live oocytes were embedded in a collagen gel to stop movement of the overall cell during measurements. Collagen gel was made by mixing M2 medium (33.5μL), 1X PBS (10 μL), NaOH (1M, 0.9 μL), collagen (3.6 mg/mL, 55.6 μL) to obtain 100 μL of the final collagen solution at 2 mg/mL with a pH$\sim$ 7.4. 20 μL of the collagen solution was deposited on a coverslip and live oocytes were added. The droplet was covered with another glass coverslip using Dow Corning vacuum grease to minimize evaporation. The collagen gel containing oocytes was polymerized in a humid environment at 37° C for 30 minutes.

5.2 Fmn2-/- and Myosin-V dominant negative

To study the effect of the actin-myosin-V network we utilize two conditions to independently perturb the actin cytoskeleton (Fmn-/-) and the myosin-V activity (MyoV(-)). Fmn-/- mouse oocytes lack cytoplasmic actin filaments, as confirmed by several independent studies [16, 17, 69, 19]. The absence of actin filaments has also been confirmed via cytochalasin-D treated mouse oocytes which exhibit the same phenotype as Fmn-/- [70]. For myosin-V dominant negative experiments (MyoV(-)), oocytes were injected with cRNAs using an Eppendorf Femtoject microinjector as published previously [20]. Oocytes were kept in prophase-I arrest for 1-3 hours to allow expression of fusion proteins. The myosin-Vb dominant negative construct corresponds to a portion of the coiled-coil region of the myosin-Vb that mediates dimerization of the motor [11]. We believe this construct binds to the coiled-coil region of endogenous myosin-Vb resulting in impaired motor dimerization. Thus, myosin-Vb is still able to bind to vesicles and actin filaments but cannot actively

generate force. It is specific to myosin-Vb and has been shown to stop vesicle motion in mouse oocytes as efficiently as brefeldin A (BFA), which is a general traffic inhibitor [20].

5.3 In-vitro Actin Network Preparation

A bulk solution of actin monomers 120 μM (Cytoskeleton Inc.) was stored overnight in depolymerization buffer (200 μM $CaCl_2$, 500 μM DTT, 2mM Tris, 200 μM ATP). It was then polymerized at a final concentration of 24 μM actin in polymerization buffer (25 mM Imidazol, 50 mM KCl, 1mM Tris, 2 mM $MgCl_2$, 1 mM DTT, 1 mM ATP). The actin gel was polymerized between two glass coverslips at room temperature. Polystyrene beads (1 μm) were embedded for optical tweezer measurements.

5.4 Optical Tweezer Setup

The optical tweezer system utilizes a near infrared fiber laser (λ = 1064 nm, YLM-1-1064-LP, IPG, Germany) that passes through a pair of acousto-optical modulators (AA-Optoelectronics, France) to control the intensity and deflection of the trapping beam. The laser is coupled into the beam path via dichroic mirrors (ThorLabs) and focused into the object plane by a water immersion objective (60x, 1.2 NA, Olympus). The condenser is replaced by a long distance water immersion objective (40x , 0.9 NA, Olympus) to collect the light and imaged by a 1:4 telescope on a InGaAs quadrant photodiode (QPD) (G6849, Hamamatsu). The resulting signal is amplified by a custom built amplifier system (Oeffner Electronics, Germany) and digitized at a 500 kHz sampling rate and 16 bit using an analog input card (6353, National Instruments, Austin, TX, USA). All control of the experimental hardware is executed using LabVIEW (National Instruments). Optical trapping of endogenous vesicles was calibrated similarly as in [31, 71], where the high-frequency fluctuations ($f > 500$ Hz) are thermal in origin [24, 30]. For direct measurement of violation of the fluctuation dissipation theorem (FDT), laser tracking interferometry is used first to measure the spontaneous fluctuations of the vesicle, followed immediately by active microrheology to measure the mechanical properties of the local environment surrounding the vesicle.

5.5 Laser Interferometry Tracking

The position of the endogenous particle is measured by back focal plane interferometry [35]. It should be noted that deformable objects (e.g., giant unilamellar vesicles $10 - 100\mu m$) undergo shape fluctuations that will manifest in the voltage measured by the QPD [72]. For small endogenous particles ($\sim 1\mu m$), it has been confirmed that shape fluctuations are small and laser interferometry can be used to track their position with nanometer precision. This has been verified by several independent studies on mammalian cells [36], yeast [37], and hair bundles [21]. We also compare our QPD measurements and show that endogenous vesicles in mouse oocytes are indistinguishable from both: polystyrene beads in living cells, and in an index-matched 50:50 water:glycerol solution in the central linear region used for position measurement (see Fig. S4 in SI). Additionally, since the endogenous vesicles serve as nodes integrated in the cytoplasmic meshwork, they are accurate reporters of the network mechanics and fluctuations [29].

5.6 Data Analysis

In the active microrheology (AMR) experiments we apply a known force, F, to an endogenous vesicle and measure the resulting displacement, u. Using linear response theory, these are related to the material response by, $u(t) = \int_{-\infty}^{t} \chi(t-t')F(t')dt'$. In Fourier space we can directly calculate the complex response as $\tilde{\chi}(\omega) = \tilde{u}(\omega)/\tilde{F}(\omega)$. To translate the response function into a shear modulus we use the Generalized Stokes-Einstein relation, $G^* = 1/[6\pi R\tilde{\chi}(\omega)]$, to calculate the elastic and viscous shear moduli (G', G'' respectively). For AMR measurements the laser power exiting the objective was ~ 120 mW. For the spontaneous fluctuations we measure the motion, $u(t)$, of endogenous vesicles via laser interferometry (without trapping the vesicle) and calculate the power spectral density (PSD), $C(\omega) = \int \langle u(t)u(0)\rangle \exp(i\omega t)dt$, as described previously [72]. Briefly, we calculate the PSD by using MATLAB (The Mathworks, USA) to take the Fast Fourier Transform (FFT) of the vesicle position, $\tilde{u} = \mathrm{FFT}(u)$. Then the PSD is calculated as, $PSD = \frac{\tilde{u}\times\tilde{u}^*}{p\times s}$, where $*$ denotes complex conjugate, p is the number of measurement points, and s is the sampling frequency. In systems at

thermal equilibrium the response function can be calculated from the PSD via the FDT as is done for passive microrheology (PMR) [38]. For PMR measurements the laser power exiting the objective was ~ 1 mW. Due to the particle size and linear range of the QPD measurement our PMR measurements are restricted to a range of approximately 500 nm.

6 Acknowledgements

We thank Jacques Prost and Jean-Francois Joanny for helpful discussions. We thank Melina Schuh (MRC Cambridge) for providing the MyoVb tail plasmid and Amanda Remorino for critical reading of the manuscript. WWA is a recipient of post-doctoral fellowships from La Fondation Pierre-Gilles de Gennes and Marie Curie Actions. MA is a recipient of post-doctoral fellowships from the Ligue Nationale contre le Cancer and from the Labex MemoLife. MB is a recipient of an AXA Ph.D. fellowship. NSG gratefully acknowledges funding from the ISF (grant no. 580/12). MHV gratefully acknowledges the Ligue Nationale Contre le Cancer (EL/2012/LNCC/MHV). TB was supported by the French Agence Nationale de la Recherche (ANR) Grants ANR-11-JSV5-0002, and the Deutsche Forschungsgemeinschaft (DFG), Cells-in-Motion Cluster of Excellence (EXC 1003 – CiM), University of Münster, Germany.

[Figure 1 about here.]

[Figure 2 about here.]

[Figure 3 about here.]

[Figure 4 about here.]

References

[1] Jonathon Howard. Mechanical Signaling in Networks of Motor and Cytoskeletal Proteins. *Annual Review of Biophysics*, 38(1):217–234, jun 2009.

[2] L Blanchoin, R Boujemaa-Paterski, C Sykes, and J Plastino. Actin dynamics, architecture, and mechanics in cell motility. *Physiol Rev*, 94:235–63, 2014.

[3] PA Janmey and CA McCulloch. Cell mechanics: integrating cell responses to mechanical stimuli. *Annu Rev Biomed Eng*, 9:1–34, 2007.

[4] DA Fletcher and RD Mullins. Cell mechanics and the cytoskeleton. *Nature*, 463:485–92, Jan 2010.

[5] N Bowden, A Terfort, J Carbeck, and GM Whitesides. Self-Assembly of Mesoscale Objects into Ordered Two-Dimensional Arrays. *Science*, 276:233–5, Apr 1997.

[6] J Palacci, S Sacanna, AP Steinberg, DJ Pine, and PM Chaikin. Living crystals of light-activated colloidal surfers. *Science*, 339:936–40, Feb 2013.

[7] Adam J. M. Wollman, Carlos Sanchez-Cano, Helen M. J. Carstairs, Robert A. Cross, and Andrew J. Turberfield. Transport and self-organization across different length scales powered by motor proteins and programmed by DNA. *Nature Nanotech*, 9(1):44–47, nov 2013.

[8] Y Sasai. Cytosystems dynamics in self-organization of tissue architecture. *Nature*, 493:318–26, Jan 2013.

[9] S Wennekamp, S Mesecke, F Nédélec, and T Hiiragi. A self-organization framework for symmetry breaking in the mammalian embryo. *Nat Rev Mol Cell Biol*, 14:452–9, 2013.

[10] T Lecuit and PF Lenne. Cell surface mechanics and the control of cell shape, tissue patterns and morphogenesis. *Nat Rev Mol Cell Biol*, 8:633–44, 2007.

[11] M Schuh. An actin-dependent mechanism for long-range vesicle transport. *Nat Cell Biol*, 13:1431–6, 2011.

[12] Z Holubcová, G Howard, and M Schuh. Vesicles modulate an actin network for asymmetric spindle positioning. *Nat Cell Biol*, 15:937–47, 2013.

[13] M Luksza, I Queguigner, MH Verlhac, and S Brunet. Rebuilding MTOCs upon centriole loss during mouse oogenesis. *Dev Biol*, 382:48–56, 2013.

[14] V Nikolova, R Zhivkova, M Markova, T Topouzova-Hristova, A Mitkova, and S Delimitreva. Characterization of mouse oocytes and oocyte-cumulus complexes extracted for nuclear matrix and intermediate filaments (NM-IF). *Acta Morph. Anthropol*, 19:149–152, 2012.

[15] M Almonacid, MÉ Terret, and MH Verlhac. Actin-based spindle positioning: new insights from female gametes. *J Cell Sci*, 127:477–83, 2014.

[16] J Azoury, KW Lee, V Georget, P Rassinier, B Leader, and MH Verlhac. Spindle positioning in mouse oocytes relies on a dynamic meshwork of actin filaments. *Curr Biol*, 18:1514–9, Oct 2008.

[17] M Schuh and J Ellenberg. A new model for asymmetric spindle positioning in mouse oocytes. *Curr Biol*, 18:1986–92, Dec 2008.

[18] D Clift and M Schuh. Restarting life: fertilization and the transition from meiosis to mitosis. *Nat Rev Mol Cell Biol*, 14:549–62, 2013.

[19] A Chaigne, C Campillo, NS Gov, R Voituriez, J Azoury, C Umaña-Diaz, M Almonacid, I Queguiner, P Nassoy, C Sykes, MH Verlhac, and ME Terret. A soft cortex is essential for asymmetric spindle positioning in mouse oocytes. *Nat Cell Biol*, 15:958–66, 2013.

[20] M Almonacid, WW Ahmed, M Bussonnier, P Mailly, T Betz, R Voituriez, NS Gov, and MH Verlhac. Active diffusion positions the nucleus in mouse oocytes. *Nat Cell Biol*, 17:470–9, 2015.

[21] P Martin, AJ Hudspeth, and F Jülicher. Comparison of a hair bundle's spontaneous oscillations with its response to mechanical stimulation reveals the underlying active process. *Proc Natl Acad Sci U S A*, 98:14380–5, 2001.

[22] AW Lau, BD Hoffman, A Davies, JC Crocker, and TC Lubensky. Microrheology, stress fluctuations, and active behavior of living cells. *Phys Rev Lett*, 91:198101, 2003.

[23] D Mizuno, C Tardin, CF Schmidt, and FC Mackintosh. Nonequilibrium mechanics of active cytoskeletal networks. *Science*, 315:370–3, Jan 2007.

[24] M Guo, AJ Ehrlicher, MH Jensen, M Renz, JR Moore, RD Goldman, J Lippincott-Schwartz, FC Mackintosh, and DA Weitz. Probing the stochastic, motor-driven properties of the cytoplasm using force spectrum microscopy. *Cell*, 158:822–32, Aug 2014.

[25] François Gallet, Delphine Arcizet, Pierre Bohec, and Alain Richert. Power spectrum of out-of-equilibrium forces in living cells: amplitude and frequency dependence. *Soft Matter*, 5(15):2947, 2009.

[26] P Bursac, G Lenormand, B Fabry, M Oliver, DA Weitz, V Viasnoff, JP Butler, and JJ Fredberg. Cytoskeletal remodelling and slow dynamics in the living cell. *Nat Mater*, 4:557–61, 2005.

[27] C Wilhelm. Out-of-equilibrium microrheology inside living cells. *Phys Rev Lett*, 101:028101, Jul 2008.

[28] D. Mizuno, D. A. Head, F. C. MacKintosh, and C. F. Schmidt. Active and Passive Microrheology in Equilibrium and Nonequilibrium Systems. *Macromolecules*, 41(19):7194–7202, oct 2008.

[29] MT Valentine, ZE Perlman, ML Gardel, JH Shin, P Matsudaira, TJ Mitchison, and DA Weitz. Colloid surface chemistry critically affects multiple particle tracking measurements of biomaterials. *Biophys J*, 86:4004–14, Jun 2004.

[30] N Fakhri, AD Wessel, C Willms, M Pasquali, DR Klopfenstein, FC MacKintosh, and CF Schmidt. High-resolution mapping of intracellular fluctuations using carbon nanotubes. *Science*, 344:1031–5, May 2014.

[31] J Mas, AC Richardson, SN Reihani, LB Oddershede, and K Berg-Sørensen. Quantitative determination of optical trapping strength and viscoelastic moduli inside living cells. *Phys Biol*, 10:046006, 2013.

[32] FC MacKintosh, J Käs, and PA Janmey. Elasticity of semiflexible biopolymer networks. *Phys Rev Lett*, 75:4425–4428, Dec 1995.

[33] David C. Morse. Viscoelasticity of Concentrated Isotropic Solutions of Semiflexible Polymers. 2. Linear Response. *Macromolecules*, 31(20):7044–7067, oct 1998.

[34] M. L. Gardel, M. T. Valentine, J. C. Crocker, A. R. Bausch, and D. A. Weitz. Microrheology of Entangled F-Actin Solutions. *Phys. Rev. Lett.*, 91(15), oct 2003.

[35] F Gittes and CF Schmidt. Interference model for back-focal-plane displacement detection in optical tweezers. *Opt Lett*, 23:7–9, 1998.

[36] S Yamada, D Wirtz, and SC Kuo. Mechanics of living cells measured by laser tracking microrheology. *Biophys J*, 78:1736–47, Apr 2000.

[37] Iva Marija Tolić-Nørrelykke, Emilia-Laura Munteanu, Genevieve Thon, Lene Oddershede, and Kirstine Berg-Sørensen. Anomalous Diffusion in Living Yeast Cells. *Phys. Rev. Lett.*, 93(7), aug 2004.

[38] R Kubo. The fluctuation-dissipation theorem. *Rep. Prog. Phys.*, 29(1):255–284, jan 1966.

[39] WW Ahmed, É Fodor, and T Betz. Active cell mechanics: Measurement and theory. *Biochim Biophys Acta*, May 2015.

[40] É. Fodor, M. Guo, N. S. Gov, P. Visco, D. A. Weitz, and F. van Wijland. Activity-driven fluctuations in living cells. *EPL*, 110(4):48005, may 2015.

[41] T Betz, M Lenz, JF Joanny, and C Sykes. ATP-dependent mechanics of red blood cells. *Proc Natl Acad Sci U S A*, 106:15320–5, 2009.

[42] E Ben-Isaac, Y Park, G Popescu, FL Brown, NS Gov, and Y Shokef. Effective temperature of red-blood-cell membrane fluctuations. *Phys Rev Lett*, 106:238103, Jun 2011.

[43] J Prost, JF Joanny, and JM Parrondo. Generalized fluctuation-dissipation theorem for steady-state systems. *Phys Rev Lett*, 103:090601, Aug 2009.

[44] É Fodor, K Kanazawa, H Hayakawa, P Visco, and Wijland F van. Energetics of active fluctuations in living cells. *Phys Rev E Stat Nonlin Soft Matter Phys*, 90:042724, 2014.

[45] AW Lau and TC Lubensky. Fluctuating hydrodynamics and microrheology of a dilute suspension of swimming bacteria. *Phys Rev E Stat Nonlin Soft Matter Phys*, 80:011917, 2009.

[46] FC MacKintosh and AJ Levine. Nonequilibrium mechanics and dynamics of motor-activated gels. *Phys Rev Lett*, 100:018104, Jan 2008.

[47] Alex J. Levine and F. C. MacKintosh. The Mechanics and Fluctuation Spectrum of Active Gels †. *J. Phys. Chem. B*, 113(12):3820–3830, mar 2009.

[48] Damien Robert, Thi-Hanh Nguyen, François Gallet, and Claire Wilhelm. In Vivo Determination of Fluctuating Forces during Endosome Trafficking Using a Combination of Active and Passive Microrheology. *PLoS ONE*, 5(4):e10046, apr 2010.

[49] D Robert, TH Nguyen, F Gallet, and C Wilhelm. In vivo determination of fluctuating forces during endosome trafficking using a combination of active and passive microrheology. *PLoS One*, 5:e10046, 2010.

[50] M Rief, RS Rock, AD Mehta, MS Mooseker, RE Cheney, and JA Spudich. Myosin-V stepping kinetics: a molecular model for processivity. *Proc Natl Acad Sci U S A*, 97:9482–6, Aug 2000.

[51] AD Mehta, RS Rock, M Rief, JA Spudich, MS Mooseker, and RE Cheney. Myosin-V is a processive actin-based motor. *Nature*, 400:590–3, 1999.

[52] G Cappello, P Pierobon, C Symonds, L Busoni, JC Gebhardt, M Rief, and J Prost. Myosin V stepping mechanism. *Proc Natl Acad Sci U S A*, 104:15328–33, Sep 2007.

[53] C Veigel, S Schmitz, F Wang, and JR Sellers. Load-dependent kinetics of myosin-V can explain its high processivity. *Nat Cell Biol*, 7:861–9, 2005.

[54] S Uemura, H Higuchi, AO Olivares, La Cruz EM De, and S Ishiwata. Mechanochemical coupling of two substeps in a single myosin V motor. *Nat Struct Mol Biol*, 11:877–83, 2004.

[55] JR Sellers and C Veigel. Direct observation of the myosin-Va power stroke and its reversal. *Nat Struct Mol Biol*, 17:590–5, 2010.

[56] C Veigel, F Wang, ML Bartoo, JR Sellers, and JE Molloy. The gated gait of the processive molecular motor, myosin V. *Nat Cell Biol*, 4:59–65, 2002.

[57] Toshihiro Toyota, David A. Head, Christoph F. Schmidt, and Daisuke Mizuno. Non-Gaussian athermal fluctuations in active gels. *Soft Matter*, 7(7):3234, 2011.

[58] R. W. Ogden and D. G. Roxburgh. A pseudo-elastic model for the Mullins effect in filled rubber. *Proceedings of the Royal Society A: Mathematical Physical and Engineering Sciences*, 455(1988):2861–2877, aug 1999.

[59] KM Schmoller, P Fernández, RC Arevalo, DL Blair, and AR Bausch. Cyclic hardening in bundled actin networks. *Nat Commun*, 1:134, 2010.

[60] MP Murrell and ML Gardel. F-actin buckling coordinates contractility and severing in a biomimetic actomyosin cortex. *Proc Natl Acad Sci U S A*, 109:20820–5, Dec 2012.

[61] N Kikuchi, A Ehrlicher, D Koch, JA Käs, S Ramaswamy, and M Rao. Buckling, stiffening, and negative dissipation in the dynamics of a biopolymer in an active medium. *Proc Natl Acad Sci U S A*, 106:19776–9, Nov 2009.

[62] Yali Yang, Jun Lin, Bugra Kaytanli, Omar A. Saleh, and Megan T. Valentine. Direct correlation between creep compliance and deformation in entangled and sparsely crosslinked microtubule networks. *Soft Matter*, 8(6):1776–1784, 2012.

[63] CJ Chan, AE Ekpenyong, S Golfier, W Li, KJ Chalut, O Otto, J Elgeti, J Guck, and F Lautenschläger. Myosin II Activity Softens Cells in Suspension. *Biophys J*, 108:1856–69, Apr 2015.

[64] WA Lam, O Chaudhuri, A Crow, KD Webster, TD Li, A Kita, J Huang, and DA Fletcher. Mechanics and contraction dynamics of single platelets and implications for clot stiffening. *Nat Mater*, 10:61–6, Jan 2011.

[65] M Guo, AJ Ehrlicher, S Mahammad, H Fabich, MH Jensen, JR Moore, JJ Fredberg, RD Goldman, and DA Weitz. The role of vimentin intermediate filaments in cortical and cytoplasmic mechanics. *Biophys J*, 105:1562–8, 2013.

[66] MJ Tyska and DM Warshaw. The myosin power stroke. *Cell Motil Cytoskeleton*, 51:1–15, 2002.

[67] MH Verlhac, JZ Kubiak, HJ Clarke, and B Maro. Microtubule and chromatin behavior follow MAP kinase activity but not MPF activity during meiosis in mouse oocytes. *Development*, 120:1017–25, 1994.

[68] A Reis, HY Chang, M Levasseur, and KT Jones. APCcdh1 activity in mouse oocytes prevents entry into the first meiotic division. *Nat Cell Biol*, 8:539–40, 2006.

[69] S Pfender, V Kuznetsov, S Pleiser, E Kerkhoff, and M Schuh. Spire-type actin nucleators cooperate with Formin-2 to drive asymmetric oocyte division. *Curr Biol*, 21:955–60, Jun 2011.

[70] J Dumont, K Million, K Sunderland, P Rassinier, H Lim, B Leader, and MH Verlhac. Formin-2 is required for spindle migration and for the late steps of cytokinesis in mouse oocytes. *Dev Biol*, 301:254–65, Jan 2007.

[71] BH Blehm, TA Schroer, KM Trybus, YR Chemla, and PR Selvin. In vivo optical trapping indicates kinesin's stall force is reduced by dynein during intracellular transport. *Proc Natl Acad Sci U S A*, 110:3381–6, Feb 2013.

[72] Timo Betz and Cécile Sykes. Time resolved membrane fluctuation spectroscopy. *Soft Matter*, 8(19):5317, 2012.

List of Figures

1 **Intracellular mechanics surrounding endogenous vesicles in living oocytes.** (A) Mouse oocytes are large spherical cells that have a well separated cortex and cytoplasmic-skeleton composed of biopolymer filaments (brightfield image, left)(scalebar = 20 μm). During prophase-I it contains a dynamic actin-myosin-V meshwork that drives vesicle motion (schematic shown in center and fluorescent image of actin filaments on right)(scalebar = 5 μm). Endogenous vesicles embedded in the cytoplasmic-skeleton are trapped using optical tweezers(zoomed inset). (B) Once a vesicle is trapped, the mechanical properties of the local environment can be measured by active microrheology (AMR) where a sinusoidal oscillating force is applied to the vesicle (blue) and the resulting displacement of the vesicle is measured (green). The viscoelastic shear modulus (G^*) is calculated from this force-displacement measurement via the Generalized Stokes-Einstein relation. (C) The mechanical properties surrounding vesicles in the cytoplasmic-skeleton of oocytes (blue) exhibits power-law behavior similar to reconstituted actin gels (gray) with frequency scaling $G^* \propto f^{0.75}$ except significantly stiffer. This shows that the cytoplasmic-skeleton in oocytes can be modeled as a semi-flexible polymer network. 17

2 **The cytoplasmic-skeleton of mouse oocytes is viscoelastic.** (A, B) Insets indicate that G' quantifies the elasticity and G'' quantifies the viscous dissipation of the cytoplasmic-skeleton. The local mechanical properties (elastic and viscous) surrounding vesicles does not change from WT (blue, $\circ$) when actin (red $\square$) or microtubules (magenta *) are absent. However, when myosin-V is inactivated (gray $\triangle$), the cytoplasmic-skeleton stiffens significantly (Kolmolgorov-Smirnov test, $p < 1 \times 10^{-7}$), showing that the activity driven dynamics of the actin-myosin-V meshwork maintains the soft mechanical environment surrounding vesicles in oocytes. (C) The ratio of the elastic and viscous moduli (G'/G'') in all oocytes shows that the cytoplasmic-skeleton is more elastic at lower frequencies and more viscous at higher frequencies with a crossover around $\sim 10 - 20$ Hz. This shows the highly viscoelastic nature of the oocyte cytoplasmic-skeleton. (sample size = WT: 11 cells, 32 vesicles; Fmn2: 10 cells, 33 vesicles; MyoV(-): 23 cells, 69 vesicles; Noc(1μM): 8 cells, 52 vesicles; shaded region indicates SEM) (note: data at 10 Hz in panel A and B are presented in a different context in [20]) 18

3 **Active force generation by myosin-V drives the cytoplasmic-skeleton out-of-equilibrium.** (A) The spontaneous motion of vesicles in oocytes (green circles) is larger than expected at thermal equilibrium (blue circles) at frequencies below 300 Hz showing that active forces are contributing to vesicle motion as highlighted by the red shaded region. This is direct evidence of nonequilibrium behavior in the cytoplasmic-skeleton (via violation of the fluctuation-dissipation theorem (FDT)). At high frequencies the observed vesicle motion resembles thermal motion indicated by the blue shaded region. (B) WT oocytes (blue) are the furthest from equilibrium as shown by their higher effective energy. In the absence of actin (red) or when myosin-V is inactivated (black) the dynamic actin-myosin-V meshwork is compromised and oocytes have lower effective energy. Solid lines are theoretical fits (equations in SI, error bars = SEM). (C) The cell force spectrum (S_{cell}) experienced by vesicles is the sum of thermal forces (S_{therm}) and active forces (S_{active}) generated by molecular motors. At high frequencies S_{cell} (green) is dominated by S_{therm} (blue) and the two spectra coincide (blue shaded region). At lower frequencies S_{cell} is larger than S_{therm} showing the existence of additional active forces. Solid lines are theoretical predictions (equations in SI), low-frequency deviation is due to simple power-law model. (D) The mean-squared-displacement (MSD) of vesicles indicates they undergo random-confined motion in the oocyte cytoplasmic-skeleton at short timescales. This behavior transitions to active diffusion at longer times [20], and is reminiscent of cytoplasmic stirring [30]. (E) When a representative trajectory (black) is filtered to remove the high-frequency thermal fluctuations the result is a smoothed trajectory (green) that represents actively driven motion. The difference between the true trajectory (gray) and the smoothed trajectory (green) recovers the high-frequency thermal fluctuations (blue) shown in (F). . . . 19

4 **A theoretical model of active mechanics connects in vivo measurements to molecular force kinetics.** (A) Vesicles (dark gray) are embedded in the complex mechanical continuum (gray background) of the oocyte interior. Actin filaments emanate from the the surface of vesicles creating an entangled network (green, left). Myosin-V motors generate force on actin (magenta, right) giving rise to forces throughout the network driving vesicles in random directions. (B) We model vesicles embedded in a mechanical continuum with local stiffness (κ) represented by the blue harmonic potential, viscoelastic dissipation (ζ_α, α), and thermal fluctuations (ξ) (left). Molecular motor activity generates an active force (f_A) through bursts of motion (v_A) and drive motion of vesicles (inset indicates motor kinetics). (C) The active force spectrum (S_{active}) quantifies the forces on vesicles due to only active processes. Combined with our quantitative model we find that the vesicles are subject to 0.4 pN of force, during a power-stroke of length $\Delta x \sim 20$ nm and duration 300 μs, resulting in a vesicle velocity of 320 nm/s, which is strikingly similar to the kinetics measured for single molecule myosin-V in-vitro and the in-vivo vesicle velocity. The solid line is the theoretical fit (equation 3), and the dotted line is a $-4/3$ power-law consistent with the cytoplasmic-skeleton mechanics. (D) Simulated vesicle motion (green squares) agrees with experimental data (blue circles) for a wide range of timescales as shown by the probability distribution of displacements. This includes long timescale ($t_{\text{pdf}} = 1$ s) Gaussian behavior and short timescale ($t_{\text{pdf}} = 0.01$ s) non-Gaussian tails (indicated by red-shaded regions) that are indicative of molecular motor behavior, where t_{pdf} is the time-lag for calculation of the displacement correlations. Gaussian distributions shown in black. These results show that molecular level kinetics of active processes can be extracted from mesoscopic in-vivo measurements. 20

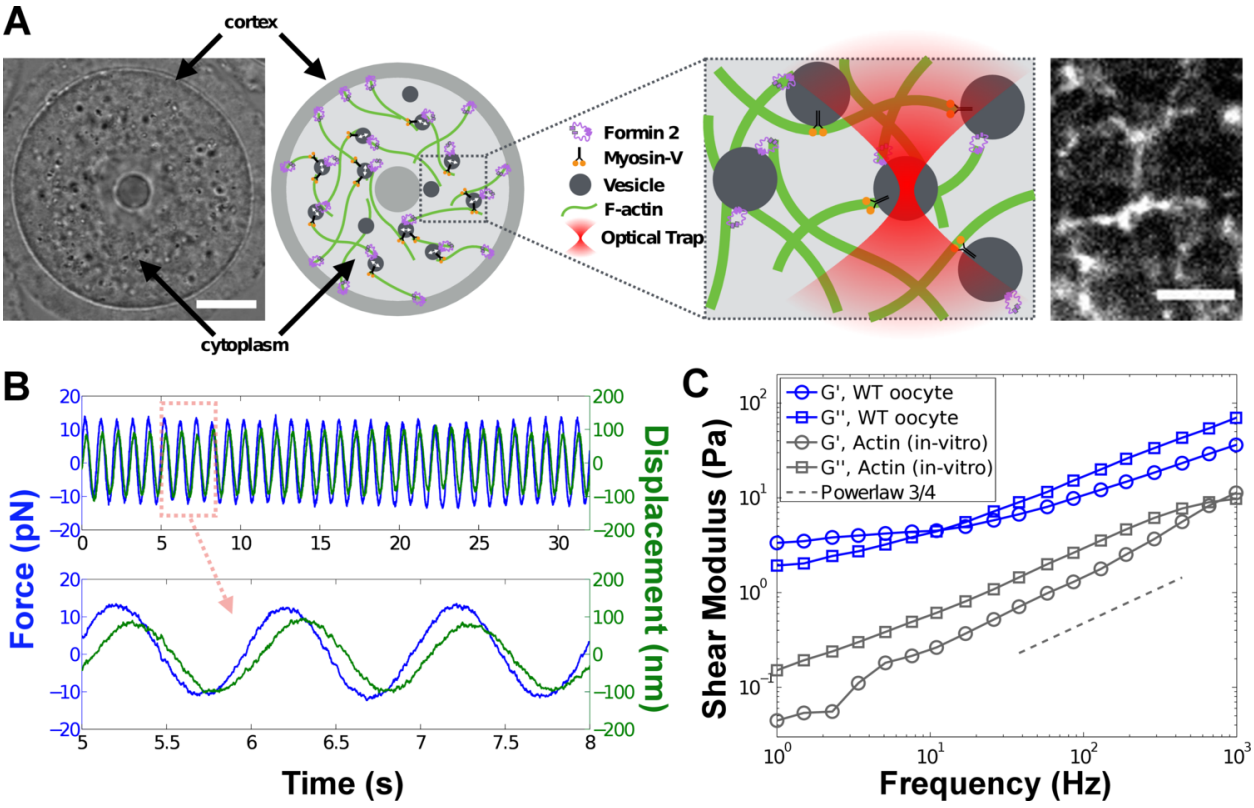

Figure 1: **Intracellular mechanics surrounding endogenous vesicles in living oocytes.** (A) Mouse oocytes are large spherical cells that have a well separated cortex and cytoplasmic-skeleton composed of biopolymer filaments (brightfield image, left)(scalebar = 20 μm). During prophase-I it contains a dynamic actin-myosin-V meshwork that drives vesicle motion (schematic shown in center and fluorescent image of actin filaments on right)(scalebar = 5 μm). Endogenous vesicles embedded in the cytoplasmic-skeleton are trapped using optical tweezers(zoomed inset). (B) Once a vesicle is trapped, the mechanical properties of the local environment can be measured by active microrheology (AMR) where a sinusoidal oscillating force is applied to the vesicle (blue) and the resulting displacement of the vesicle is measured (green). The viscoelastic shear modulus (G^*) is calculated from this force-displacement measurement via the Generalized Stokes-Einstein relation. (C) The mechanical properties surrounding vesicles in the cytoplasmic-skeleton of oocytes (blue) exhibits power-law behavior similar to reconstituted actin gels (gray) with frequency scaling $G^* \propto f^{0.75}$ except significantly stiffer. This shows that the cytoplasmic-skeleton in oocytes can be modeled as a semi-flexible polymer network.

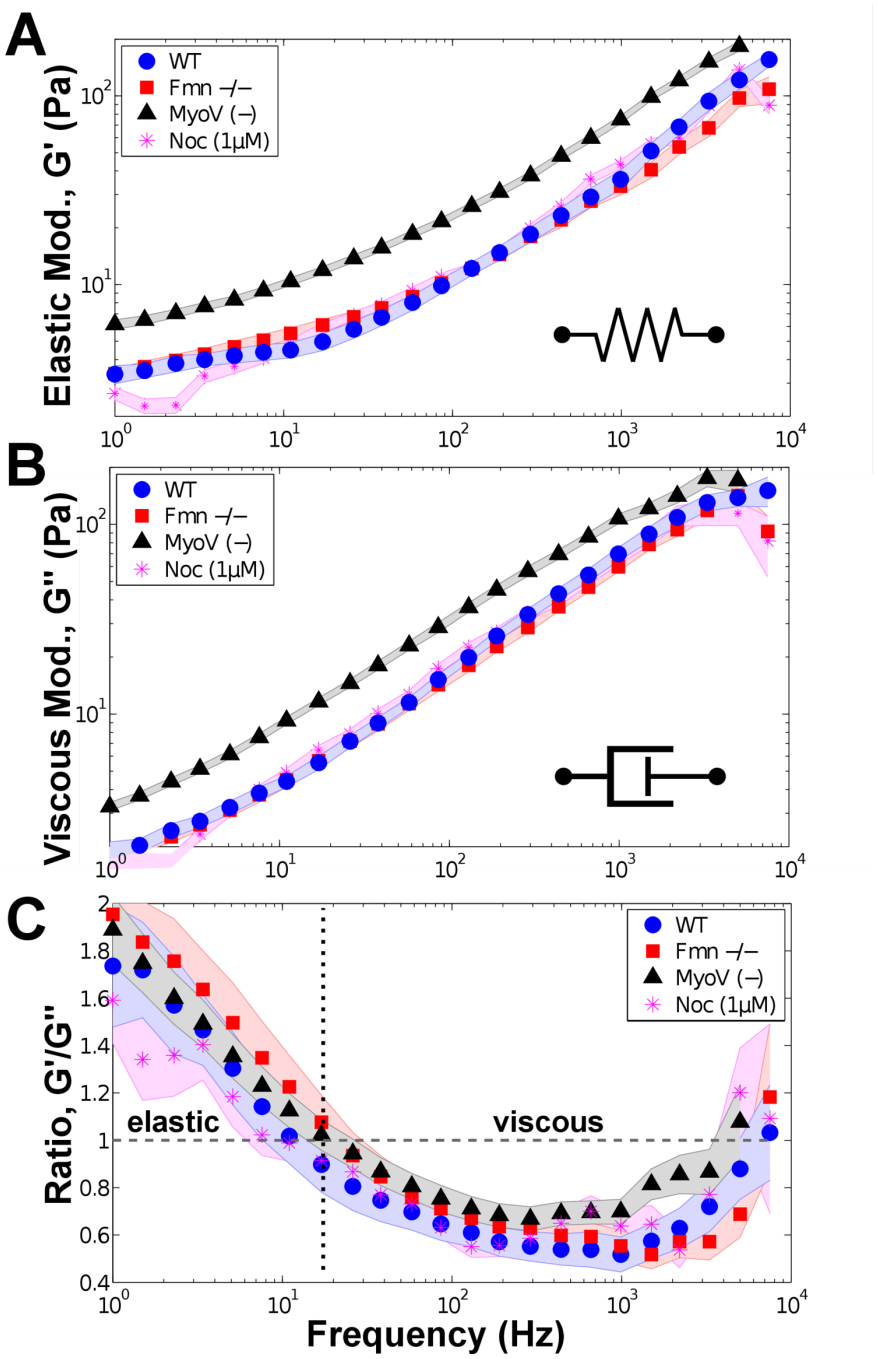

Figure 2: **The cytoplasmic-skeleton of mouse oocytes is viscoelastic.** (A, B) Insets indicate that G' quantifies the elasticity and G'' quantifies the viscous dissipation of the cytoplasmic-skeleton. The local mechanical properties (elastic and viscous) surrounding vesicles does not change from WT (blue, ∘) when actin (red □) or microtubules (magenta *) are absent. However, when myosin-V is inactivated (gray △), the cytoplasmic-skeleton stiffens significantly (Kolmolgorov-Smirnov test, $p < 1\times10^{-7}$), showing that the activity driven dynamics of the actin-myosin-V meshwork maintains the soft mechanical environment surrounding vesicles in oocytes. (C) The ratio of the elastic and viscous moduli (G'/G'') in all oocytes shows that the cytoplasmic-skeleton is more elastic at lower frequencies and more viscous at higher frequencies with a crossover around $\sim 10-20$ Hz. This shows the highly viscoelastic nature of the oocyte cytoplasmic-skeleton. (sample size = WT: 11 cells, 32 vesicles; Fmn2: 10 cells, 33 vesicles; MyoV(-): 23 cells, 69 vesicles; Noc(1μM): 8 cells, 52 vesicles; shaded region indicates SEM) (note: data at 10 Hz in panel A and B are presented in a different context in [20])

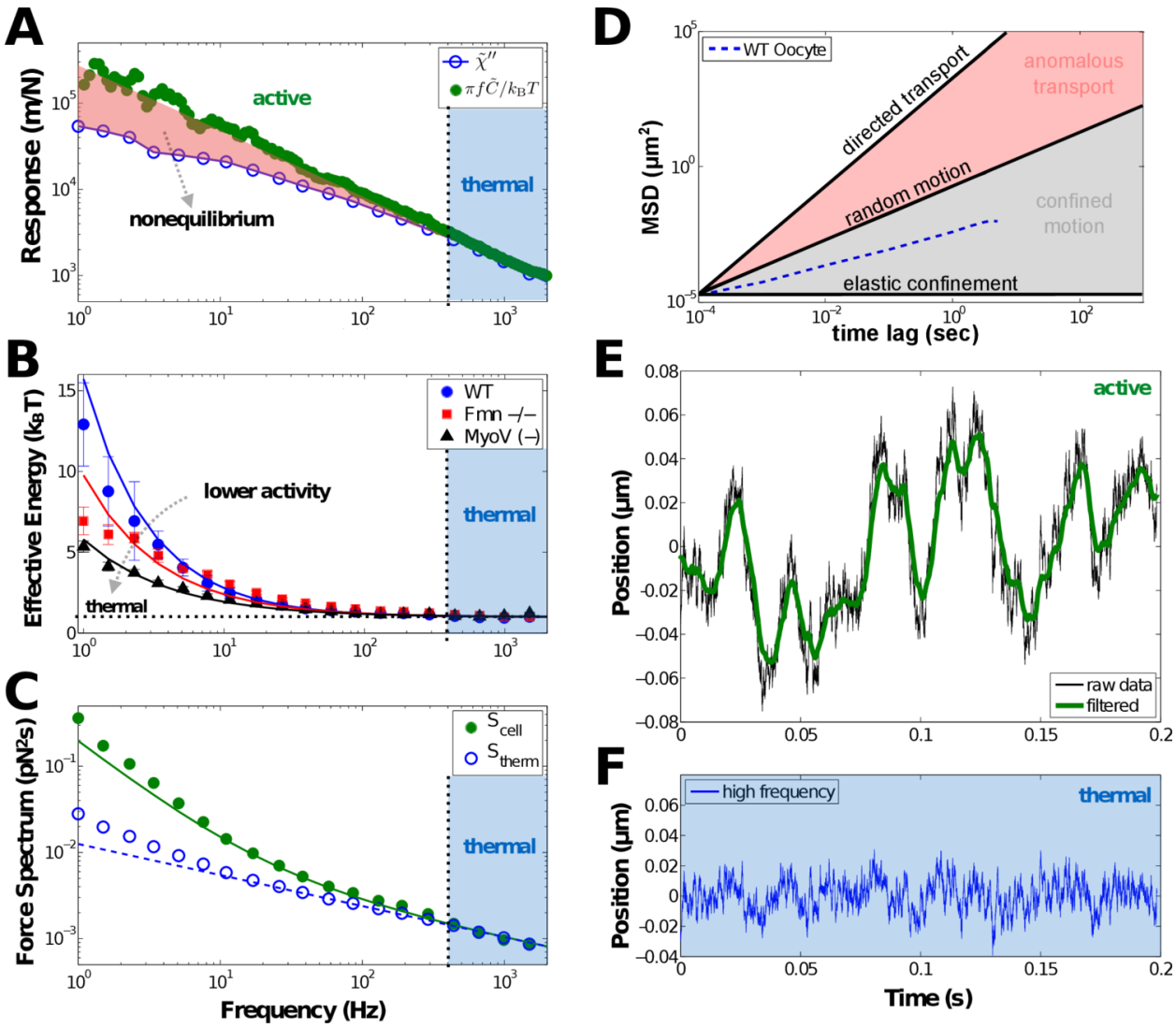

Figure 3: **Active force generation by myosin-V drives the cytoplasmic-skeleton out-of-equilibrium.** (A) The spontaneous motion of vesicles in oocytes (green circles) is larger than expected at thermal equilibrium (blue circles) at frequencies below 300 Hz showing that active forces are contributing to vesicle motion as highlighted by the red shaded region. This is direct evidence of nonequilibrium behavior in the cytoplasmic-skeleton (via violation of the fluctuation-dissipation theorem (FDT)). At high frequencies the observed vesicle motion resembles thermal motion indicated by the blue shaded region. (B) WT oocytes (blue) are the furthest from equilibrium as shown by their higher effective energy. In the absence of actin (red) or when myosin-V is inactivated (black) the dynamic actin-myosin-V meshwork is compromised and oocytes have lower effective energy. Solid lines are theoretical fits (equations in SI, error bars = SEM). (C) The cell force spectrum ($S_{\rm cell}$) experienced by vesicles is the sum of thermal forces ($S_{\rm therm}$) and active forces ($S_{\rm active}$) generated by molecular motors. At high frequencies $S_{\rm cell}$ (green) is dominated by $S_{\rm therm}$ (blue) and the two spectra coincide (blue shaded region). At lower frequencies $S_{\rm cell}$ is larger than $S_{\rm therm}$ showing the existence of additional active forces. Solid lines are theoretical predictions (equations in SI), low-frequency deviation is due to simple power-law model. (D) The mean-squared-displacement (MSD) of vesicles indicates they undergo random-confined motion in the oocyte cytoplasmic-skeleton at short timescales. This behavior transitions to active diffusion at longer times [20], and is reminiscent of cytoplasmic stirring [30]. (E) When a representative trajectory (black) is filtered to remove the high-frequency thermal fluctuations the result is a smoothed trajectory (green) that represents actively driven motion. The difference between the true trajectory (gray) and the smoothed trajectory (green) recovers the high-frequency thermal fluctuations (blue) shown in (F).

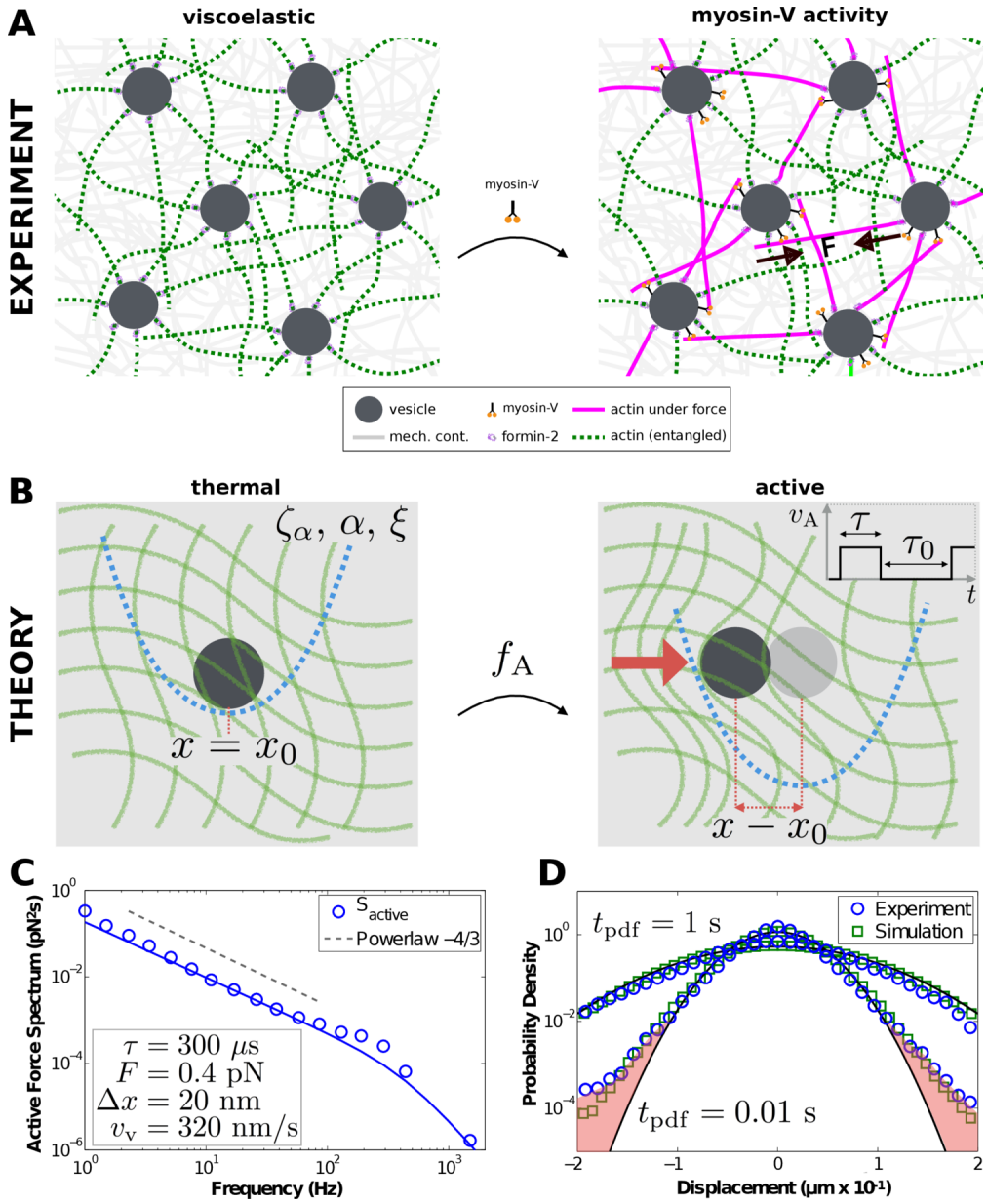

Figure 4: **A theoretical model of active mechanics connects in vivo measurements to molecular force kinetics.** (A) Vesicles (dark gray) are embedded in the complex mechanical continuum (gray background) of the oocyte interior. Actin filaments emanate from the the surface of vesicles creating an entangled network (green, left). Myosin-V motors generate force on actin (magenta, right) giving rise to forces throughout the network driving vesicles in random directions. (B) We model vesicles embedded in a mechanical continuum with local stiffness (κ) represented by the blue harmonic potential, viscoelastic dissipation (ζ_α, α), and thermal fluctuations (ξ) (left). Molecular motor activity generates an active force (f_A) through bursts of motion (v_A) and drive motion of vesicles (inset indicates motor kinetics). (C) The active force spectrum (S_{active}) quantifies the forces on vesicles due to only active processes. Combined with our quantitative model we find that the vesicles are subject to 0.4 pN of force, during a power-stroke of length $\Delta x \sim 20$ nm and duration 300 μs, resulting in a vesicle velocity of 320 nm/s, which is strikingly similar to the kinetics measured for single molecule myosin-V in-vitro and the in-vivo vesicle velocity. The solid line is the theoretical fit (equation 3), and the dotted line is a $-4/3$ power-law consistent with the cytoplasmic-skeleton mechanics. (D) Simulated vesicle motion (green squares) agrees with experimental data (blue circles) for a wide range of timescales as shown by the probability distribution of displacements. This includes long timescale ($t_{\text{pdf}} = 1$ s) Gaussian behavior and short timescale ($t_{\text{pdf}} = 0.01$ s) non-Gaussian tails (indicated by red-shaded regions) that are indicative of molecular motor behavior, where t_{pdf} is the time-lag for calculation of the displacement correlations. Gaussian distributions shown in black. These results show that molecular level kinetics of active processes can be extracted from mesoscopic in-vivo measurements.

List of Tables

1 Myosin-V force kinetics in-vivo and in-vitro 22

Table 1: Myosin-V force kinetics in-vivo and in-vitro

	in-vivo oocytes	single molecule myosin-V	reference
F(pN)	0.4	0-4	[50, 52, 51, 53]
$\tau(\mu$s)	300	160-1000	[52, 55, 54]
Δx(nm)	20	15-25	[52, 56, 55, 54]
$v_{\mathrm{v}}(\mu$m/s)	320	270-480	[51, 53, 54]